Journal of APPLIED PHYSICS

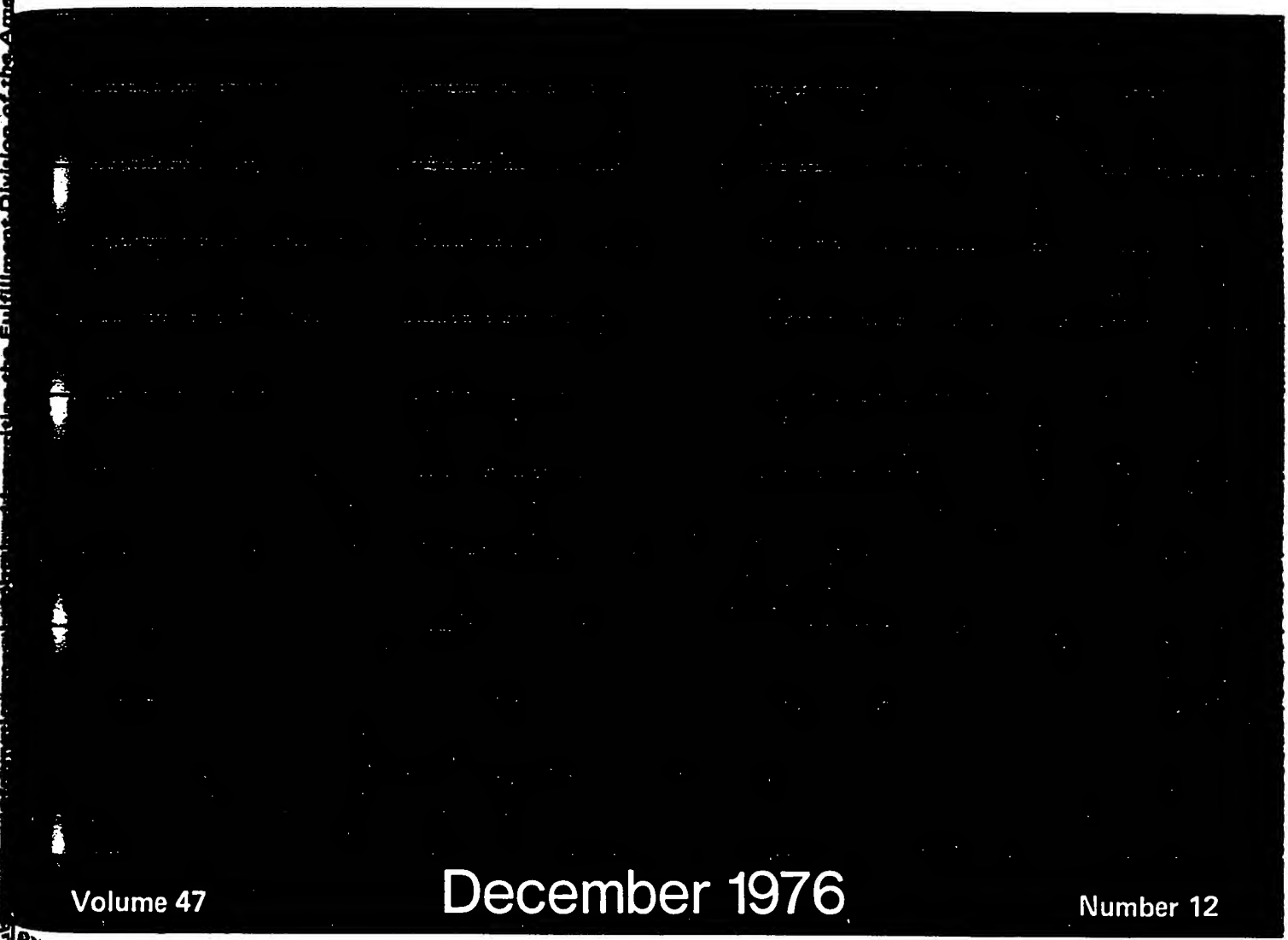

Volume 47 December 1976 Number 12

a publication of the American Institute of Physics

Journal of APPLIED PHYSICS Vol. 47, No. 12, December 1976

(Continued)

Physical properties of thin-film field emission cathodes with molybdenum cones

C. A. Spindt, I. Brodie, L. Humphrey, and E. R. Westerberg

Stanford Research Institute, Menlo Park, California 94025
(Received 18 March 1976; in final form 15 July 1976)

Field emission cathodes fabricated using thin-film techniques and electron beam microlithography are described, together with effects obtained by varying the fabrication parameters. The emission originates from the tip of molybdenum cones that are about 1.5 μm tall with a tip radius around 500 Å. Such cathodes have been produced in closely packed arrays containing 100 and 5000 cones as well as singly. Maximum currents in the range 50–150 μA per cone can be drawn with applied voltages in the range 100–300 V when operated in conventional ion-pumped vacua at pressures of 10^{-9} Torr or less. In the arrays, current densities (averaged over the array) of above 10 A/cm² have been demonstrated. Life tests with the 100-cone arrays drawing 2 mA total emission (or 3 A/cm²) have proceeded in excess of 7000 h with about a 10% drop in emission current. Studies are presented of the emission characteristics and current fluctuation phenomena. It is tentatively concluded that the emission arises from only one or a few atomic sites on the cone tips.

PACS numbers: 79.70.+q, 29.25.Bx, 52.80.Vp

I. INTRODUCTION

Several years ago Spindt and his co-workers at SRI[1,2] developed methods for fabricating arrays of minute cones for use as field emission cathodes by evolving new techniques in thin-film technology and electron beam microlithography. Since that time the technology of fabrication has been advanced, taking advantage of improvements in silicon thin-film technology instigated by the growing needs of the semiconductor industry. The technology now allows the cathodes to be made in arrays of up to 5000 cathodes at packing densities up to $6.4\times10^5/\text{cm}^2$.

Apart from the precision with which individual cones may be positioned and the ability to pack large numbers of identical cones into small areas, a major advantage offered by these cathodes is the very low voltages at which they operate. These voltages range from 100 to 300 V for useful emission, compared with values ranging from 1000 to 30 000 V for conventional etched wire emitters. This low-voltage operation is achieved by placing the accelerating electrode close to the tip and making the radius of the tip very small. The low voltage of operation of these cathodes makes them less vulnerable to damage by ionization of the ambient gas.[3] Hence, the low voltage allows the cathodes to operate continuously with very stable emission properties and long life, at pressures higher than those necessary for conventional field emitters, and without resorting to strategems of intermittent or continuous heating. Furthermore, the arrays are capable of operating at effective current densities (averaged over the area of the array) of greater than 10 A/cm² continuously, far higher than can be obtained with thermionic cathodes with a reasonable life expectancy.[4]

Molybdenum is a particularly good material to use for the sharp pointed cones, from which the electrons are emitted. A high degree of reproducibility has been achieved with this material, even though the cathodes cannot be heated to the temperatures necessary to completely remove absorbed and dissolved gases from the region of the emitting area. Molybdenum is not considered to be necessarily the ideal material for the cone, and studies are now being made using materials with lower work functions to further decrease the operating voltages. However, molybdenum has properties that are very useful in fabricating cones and a large amount of the data has been accumulated on this material. The purpose of this paper is to describe the manufacture and properties of this type of thin-film field emission cathode and compare its performance with conventional etched molybdenum cathodes.

II. DESCRIPTION OF THE TFFEC AND ITS METHOD OF FABRICATION

The thin-film field emission cathode (TFFEC) con-

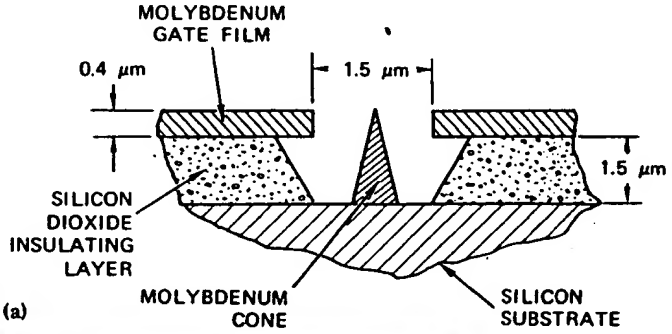

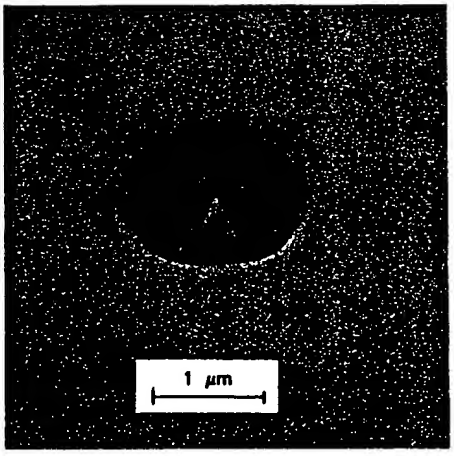

FIG. 1. Schematic diagram and scanning electron micrograph of a thin-film field emission cathode (TFFEC).

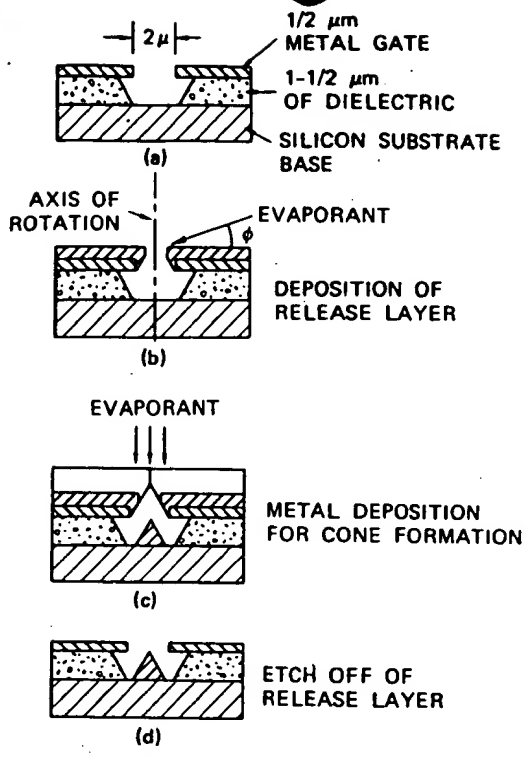

FIG. 2. Thin-film field emission cathode fabrication.

sists basically of a conductor/insulator/conductor sandwich (Fig. 1). The top conductor or gate film has holes of from 1.0 to 3 μm in diameter in it, through which a cavity can be etched in the insulator. This cavity undercuts the gate and uncovers the substrate conductor. A metal cone whose base is attached to the substrate and whose tip is close to the plane of the gate film is then formed in the cavity.

Heavily doped silicon is preferred as the substrate, since silicon dioxide can be grown on its surface to thickness of around 1 μm with excellent adherence, no porosity, and high-field breakdown strength. A film of molybdenum (about 0.4 μm thick) is vacuum deposited on the silicon dioxide to provide the gate electrode. The cone height, tip radius, and gate aperture are variables of the fabrication technique that offer some control over the current-voltage characteristic, as discussed in Sec. III D,

The present method of fabrication is as follows:

(a) Obtain standard 5-cm-diam silicon wafers, 0.75 mm thick of highly conducting (0.01 Ω/cm) silicon, as are used for semiconductor fabrication.

(b) Oxidize the wafers to the desired thickness—usually about 1.5 μm—using standard oxidation techniques.[5]

(c) Cut wafers into squares of a size suitable for handling by scribing and breaking.

(d) Coat the oxide with a uniform layer (0.4 μm thick) of molybdenum. Electron beam evaporation is more convenient for this purpose than sputtering.

(e) Coat the squares on the molybdenum side with an electron-sensitive resist, PMM (poly-methyl-methacrylate), to a thickness of about 1 μm, using standard spinning methods.[6]

(f) Expose the resist-coated surface in vacuum to a pattern of electron beams focused to form an array of spots in the desired configuration. The electron projection techniques were devised by Westerberg, and the details of these techniques are given elsewhere.[7] The exposed spots are usually about 1 μm in diameter. Square arrays on 25.4- and 12.7-μm centers have been made.

(g) Remove the PMM that has been exposed to electrons, by dissolving these areas in isopropyl alcohol, exposing the underlying molybdenum. Then, selectively etch the molybdenum through to the silicon dioxide layer.

(h) Remove the remaining PMM. Then, etch the silicon dioxide down to the silicon base with hydrofluoric acid solution. At this point, the structure takes the form illustrated in Fig. 2(a). The molybdenum layer is undercut by removal of silicon dioxide, since the acid does not attack molybdenum.

(i) Mount the substrate in a vacuum deposition system and rotate the substrate about an axis perpendicular to its surface. A parting layer of aluminum is deposited at grazing incidence. In this way the size of the holes can be decreased to any desired diameter [Fig. 2(b)].

(j) Deposit molybdenum through the partially closed holes by electron beam evaporation from a small source at normal incidence. The size of the hole continues to decrease because of condensation of molybdenum on its

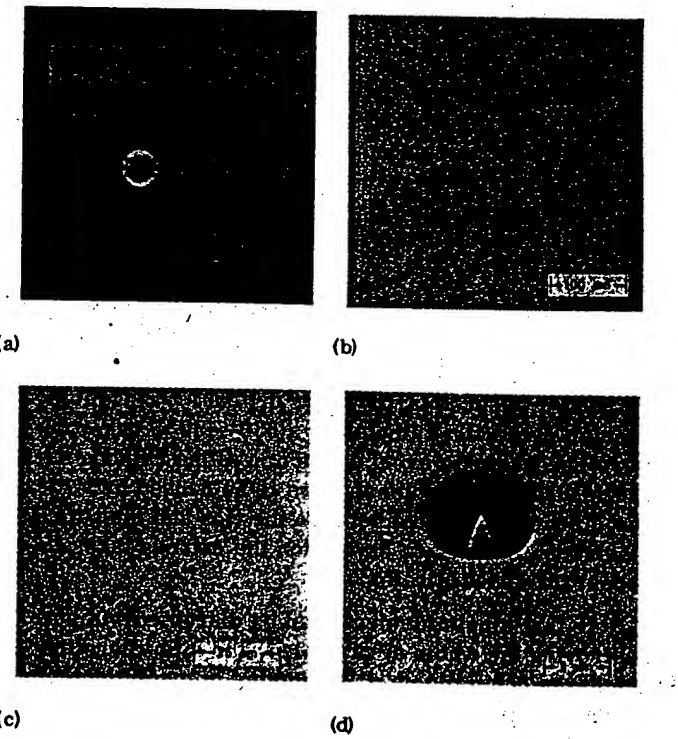

FIG. 3. An array of 5000 thin-film field emission cathodes on 0.0005 -in. centers. (a) Cathode chip mounted on a ceramic holder. (b) Portion of the 5000-tip array magnified. (c) High magnification of part of the array. (d) Ultrahigh magnification of a tip in the array.

FIG. 4. Micrograph of cathode array showing the results of sandwich breakdown between two of the cones and the gate film.

periphery. A cone grows inside the cavity as the molybdenum vapor condenses on a smaller area, limited by the decreasing size of the aperture. The point is formed as the aperture closes. Considerable control of the cone height, angle, and tip radius is obtained by choice of the starting aperture size, the thickness of oxide layer, and the distance of the evaporation source from the substrate.

(k) Dissolve the parting layer of aluminum, releasing the molybdenum film deposited during the cone formation step. After a thorough cleaning, the cathode is ready for mounting in a vacuum tube.

Using these procedures, cathodes with 1, 100, and 5000 emitting cones have been grown. The 100-cone array was arranged in a 10×10 matrix with 25.4 μm spacing, the total cathode area covering a square that is 0.25 mm on each side. The 5000-cone array was arranged in a circular area 1.0 mm in diameter, with the emitting cones placed in a rectangular matrix with 12.7 μm spacing. Figure 3 shows a 5000-cone array at various magnifications. The data shown in Figs. 3(c) and 3(d) were obtained with a scanning electron microscope.

The cathodes were mounted on a ceramic header and spaced at a suitable distance from a metal collector electrode. Tests are made in ion-pumped systems at ambient pressures of 10^{-9} Torr or less. Stringent high-vacuum procedures (including a 350—450 °C bakeout) were necessary to avoid disruption of the cathode early in life. This disruption appears to be caused by a local gas discharge forming between the tips and the gate electrode. After such disruption the cathode takes the appearance shown in Fig. 4.

Note that single elements can be disrupted without destroying the whole array. Also, the site where the discharge occurred usually remains open-circuited between the base and the gate so that the device is still operable. Outgassing of the active components of the tube, including the cathode itself, is the main source of gas for this discharge. This effect can be essentially eliminated by bombarding all the active parts of the tube (including the cathode) with electrons from a separate tungsten thermionic filament, appropriately disposed in the tube.

An important difference between the TFFEC and the conventional etched wire field emitter is that TFFEC cannot be heated to temperatures above 700 °C, due to distortion caused by the stresses set up by the different thermal expansions of the component layers. Thus, the adsorbed gases on the surface of the tip and sources for their replenishment by surface or solid diffusion are never completely removed. Furthermore, the growth of a single crystal at the tip, with the usual field/heat emission enhancement effects due to buildup at the crystal boundaries, is not evident.

Field emission micrographs from a single TFFEC point were made, and one or a few lobes were observed without regular structure. Twinkling and movement of the lobes were observed.

III. EMISSION PROPERTIES

A. Theoretical background

The generally accepted Fowler-Nordheim theory[8] for a clean metal surface relates the field emission current density, J, to the electric field at the surface, E, in volts/cm and the work function ϕ in electron volts by the equation

$$J=\frac{AE^2}{\phi t^2(y)}\exp\left(-B\frac{\phi^{3/2}}{E}v(y)\right)\frac{\text{A}}{\text{cm}^2}, \tag{1}$$

where

$$A=1.54\times10^{-6},$$

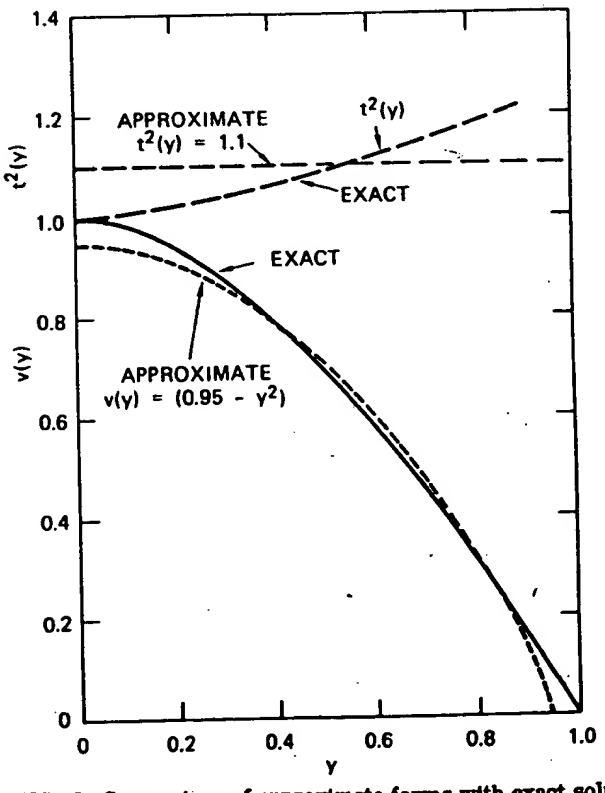

FIG. 5. Comparison of approximate forms with exact solutions for the Fowler-Nordheim field emission functions $v(y)$ and $t^2(y)$.

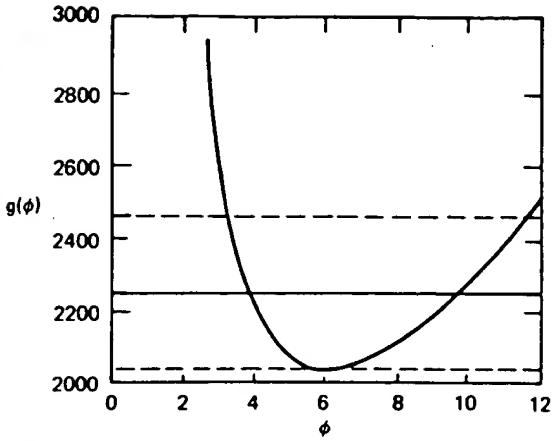

FIG. 6. $g(\phi)$ as a function of ϕ.

$$B = 6.87 \times 10^7,$$

$$y = 3.79 \times 10^{-4} E^{1/2}/\phi .$$

y is the Schottky lowering of the work-function barrier.

The functions $v(y)$ and $t(y)$ have been computed[9] and, as can be seen from Fig. 5, we can use as a close approximation over the operating range of most cathodes the following values:

$$t^2(y) = 1.1 \quad \text{and} \quad v(y) = 0.95 - y^2. \tag{3}$$

Typically, the field emission current I is measured as a function of the applied voltage V and we can substitute $J = I/\alpha$ and $E = \beta V$ in Eq. (1), where α is the emitting area and β is the local field conversion factor at the emitting surface. Combining these relationships gives

$$I = aV^2 \exp(-b/V), \tag{4}$$

where

$$a = \frac{\alpha A \beta^2}{1.1\phi} \exp\left(\frac{B(1.44 \times 10^{-7})}{\phi^{1/2}}\right), \tag{5}$$

$$b = 0.95 B \phi^{3/2}/\beta. \tag{6}$$

By differentiating Eq. (4) we obtain

$$\frac{dI}{dV} = \frac{I}{V}\left(2 + \frac{b}{V}\right). \tag{7}$$

Thus, by measuring I, V, and dI/dV at any given point on the current-voltage characteristic we may obtain the value of b at a specific current I from Eq. (7). Substitution of b/V in Eq. (4) gives a.

Since we have three unknown constants to determine in a given field emission situation—namely, α, β, and ϕ—it is impossible to separate them with a knowledge of a and b only. An independent method must be found of measuring one of them or finding some other relationship between them.

Following Van Oostrom[10] and Charbonnier and Martin,[11] we note that

$$ab^2 = \frac{(0.95)^2}{1.1} \alpha A B^2 \phi^2 \exp\left(\frac{B(1.44 \times 10^{-7})}{\phi^{1/2}}\right),$$

$$ab^2 = \alpha(5.96 \times 10^9)\phi^2 \exp(9.89/\phi^{1/2}). \tag{8}$$

The function $g(\phi) = \phi^2 \exp(9.89/\phi^{1/2})$ is plotted in Fig. 6 over the range $\phi = 1$ to $\phi = 12$. This shows that if a fixed value of $g(\phi) = 2250$ is chosen, then the error will not be greater than $\pm 10\%$ over the range $\phi = 3.4$ to $\phi = 11.6$. Fortunately, this covers the work-function range of many practical field emitters. Using the above value for $g(\phi)$ enables us to estimate the emitting area α to $\pm 10\%$ from the relation

$$\alpha = ab^2/(1.34 \times 10^{13}) \quad \text{cm}^2. \tag{9}$$

Combining Eqs. (4) and (9) we obtain

$$\frac{\alpha}{I} = \frac{(b^2/V)\exp(b/V)}{1.34 \times 10^{13}}. \tag{10}$$

This relationship is plotted in Fig. 7 for values of b/V in the range 5—15. This covers the practical range for field emission. Figure 7 shows clearly that to estimate α within a factor of 3, b/V must be obtained with a precision of better than $\pm 10\%$.

Equation (7) gives

$$\frac{b}{V} = \frac{V}{I}\frac{dI}{dV} - 2 \tag{11}$$

so that the individual measurement of V, I, and dI/dV must be precise to about 1% for this method to have an error even approaching that of Eq. (9) for the emission area. In practice dI/dV is difficult to measure with the required precision.

As can be seen from this analysis, the order of magnitude of the apparent emitting area α can be obtained by the measurement of I, V, and dI/dV, provided the cathode is aged to the point where good Fowler-Nordheim plots are obtained.

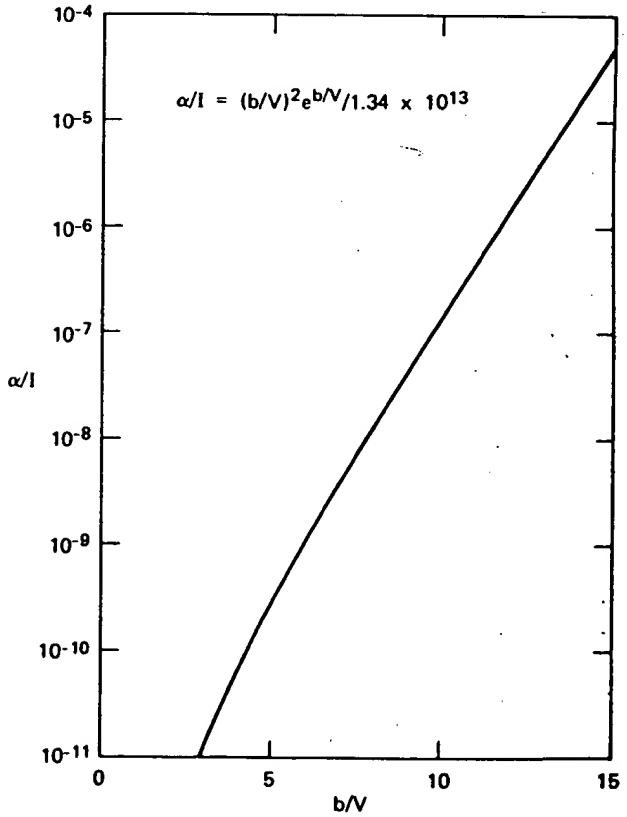

FIG. 7. α/I as a function of b/V.

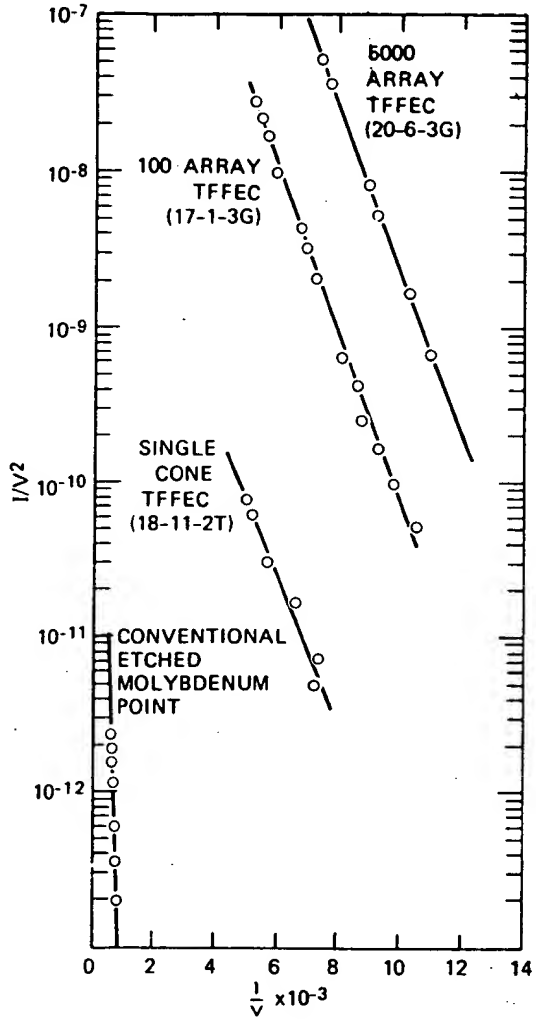

FIG. 8. Fowler-Nordheim plots for representative cathodes.

B. Current-voltage characteristics

In Fig. 8 Fowler-Nordheim plots for different varieties of cathodes—namely, single-cone TFFEC's, arrays of 100 TFFEC's, and arrays of 5000 TFFEC's—are compared with an etched molybdenum wire. The etched wire was not heat treated, so the condition of its tip was similar to that of the TFFEC cones. Etched wire emitters show considerable variability in their emission performance from one sample to another. Although they all evinced straight-line Fowler-Nordheim plots, the voltage to draw 1 μA of emission varied from 1000 to 2500 V.

As will be seen, reasonable straight lines are obtained for the TFFEC's and, in the samples chosen, are nearly parallel to each other. The displacement is approximately equal in ratio to the number of emitting points. Differences among the cathodes are attributed mainly to different dimensions in the samples of cone heights, gate hole diameters, and tip radii.

An important conclusion from these results, verified by scanning electron microscope studies, is that the individual cones in any given array must be almost identical, with a very small spread in the field conversion factor β among them. We note from Dyke and Dolan's tables[12] that a deviation of E $(=\beta V)$ of only 20% from the average would increase or decrease the emission of an individual cone by a factor of more than 10 (assuming a work function of about 4.5 eV and fields of about 5×10^{7} V/cm).

The maximum current that can be drawn from a single TFFEC tip is usually in the range 50—150 μA for a well-aged tube. If the current exceeds this value the cone completely disrupts in a manner analogous to the disruption of field emitting whiskers in vacuum breakdown.[13] Currents up to 5 mA (corresponding to an effective current density of 8 A/cm^2) have been drawn from the 100-cone arrays on 25.4-μm centers and, under pulse conditions, currents of up to 100 mA (corresponding to a current density of 12 A/cm^2) have been drawn from 5000-cone arrays on 12.7-μm centers. In the latter case the main difficulty in reaching an anticipated 50 μA $\times$5000 = 250 mA (or 30 A/cm^2) current has been associated with the anode of the tube, which was not designed to dissipate the powers involved.

C. Estimation of the emitting area

We attempted to measure the emitting area of the cones using the method described in Sec. III A. Average values of dI/dV were obtained by precise measurements of the change of I with V around the point under consideration and by using the lock-in amplifier technique. Results for the above cathodes are shown in Table I. Apparent emitting areas of the TFFEC's are of the order of 1.2×10^{-15} cm^2/cone compared to values of 160×10^{-15} and 71×10^{-15} cm^2 for two etched points.

If these results are taken at their face value, it would

TABLE I. Estimates of apparent emitting areas by the Fowler-Nordheim method.

Cathode	Number of tips (n)	V	I	$\frac{dI}{dV}$	$\frac{b}{V}$	$\frac{\alpha}{I}$	Total apparent emitting (α)	Average apparent emitting area per tip (α/n)
18-11-2T	1	139	1.92×10^{-7}	1.3×10^{-8}	7.41	7×10^{-9}	1.3×10^{-15}	1.3×10^{-15}
17-1-3G	100	136	3.0×10^{-6}	2.0×10^{-6}	7.07	4.3×10^{-9}	1.3×10^{-13}	1.3×10^{-15}
20-6-3G	5000	137	1.0×10^{-3}	7.1×10^{-5}	7.72	1.0×10^{-6}	1.0×10^{-11}	2.0×10^{-15}
Etched wire No. 1	1	2244	1.0×10^{-6}	5.4×10^{-9}	10.1	1.6×10^{-7}	1.6×10^{-13}	160×10^{-15}
Etched wire No. 2	1	1415	1.19×10^{-6}	9.5×10^{-9}	9.3	6×10^{-6}	7.1×10^{-14}	71×10^{-15}

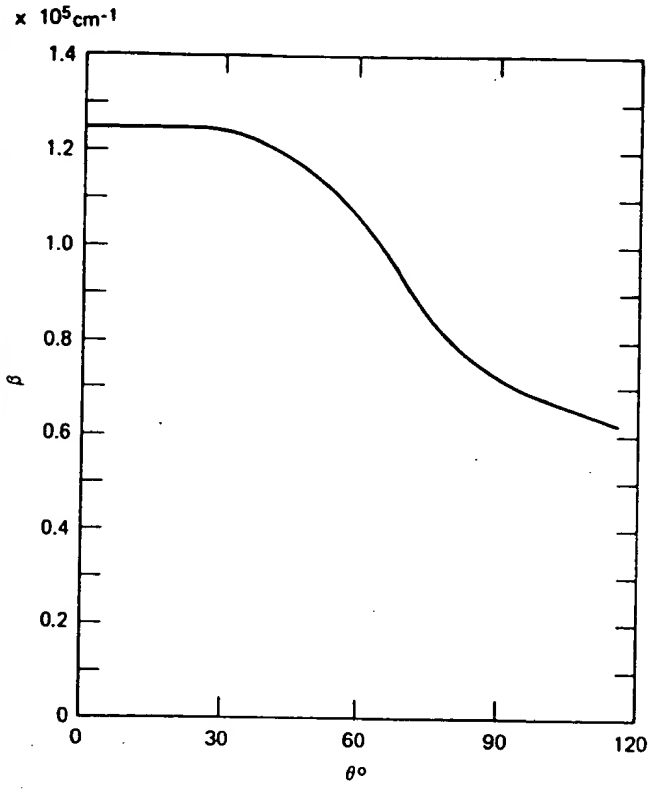

FIG. 9. Field conversion factor β as a function of the polar angle θ for the cone tip of a TFFEC.

appear that only a few atomic sites at the very tip of the cones are contributing to the emission. The observation is well known[10,14] that field emitters that have not been treated by the usual field/heat methods to clean and "build up" the tips give anomalously low areas. This phenomenon has been attributed to the fact that the surface remains contaminated with adsorbed gas. Experiments in which gas is introduced after the tip has been cleaned appears to corroborate this conclusion. Gomer (Ref. 16, p. 50) has shown that the empirical assumption of a linear variation of work function with electric field, as might be expected from an adsorbed monolayer or other surface and band structure effects, leads to an apparent reduction in emission area by a factor

$$f = \exp(3\gamma\beta b/2\phi_0) \tag{12}$$

by assuming $\phi = \phi_0 + \gamma E$, where ϕ_0 is the work function at zero field. The assumption of a linear variation of work function with field is directly analogous to the commonly assumed linear variation of work function with temperature in thermionic emission that is used to interpret the thermionic constants.[15] Gomer's derivation also shows clearly that if f were smaller than 10^{-3} this variation would begin to cause noticeable deviations from the Fowler-Nordheim law.

Due to the perfection with which the cathodes are made, we could measure the dimensions of the critical parameters that govern the field at the cone tip with considerable precision using the scanning electron microscope (SEM) down to the resolution of the instrument used, which was about 100 Å.

A representative set of dimensions (see Fig. 10) was as follows: thickness of gate electrode, $t = 0.4$ μm; diameter of hole in gate electrode: $D = 1.3$ μm; thickness of insulating layer, $d = 1.4$ μm; cone height, $h = 1.4$ μm; cone base diameter, $b = 1.0$ μm; tip radius, $r = 0.05$ μm. These dimensions were used to compute the electric field around the tip. This computation was made using a CDC 6400 digital computer and the relaxation methods to solve Laplace's equation in the interelectrode region. By using successively smaller mesh sizes, the equipotentials could be obtained to any desired degree of accuracy.

In Fig. 9 the calculated field conversion factor β is plotted as a function of the polar angle θ measured from the center of curvature of the tip. It is seen that the field is essentially constant for 30° and then begins slowly dropping off. The value of β at the center, namely, $\beta_0 = 1.25 \times 10^5$ cm^{-1}, compares with a value for an isolated sphere radius 0.05 μm with a concentric spherical anode of radius 0.65 μm of $\beta_0 = 2.17 \times 10^5$ cm^{-1}. This reduction from the isolated sphere case of a factor of 1.7 is reasonable, in view of the presence of the shank and the fact that plane-parallel electrodes are used. This compares with a reduction factor of 5 mentioned by Gomer[16] for a conventional free-standing tip with the anode essentially at infinity.

The effective emitting area can be roughly defined by the angle where the field has dropped off by 10% and the current density has been reduced by a factor of 5. Using this criterion the emitting area would be defined by a spherical cap radius of 0.05 μm and a half-angle of 53° or 6.3×10^{-11} cm^2. This area is more than 10^4 times greater than that estimated from the current-voltage characteristics. The field at the tip with 139 V applied would be 1.74×10^7 V/cm^2. To obtain 1.92×10^7 A from the above area, corresponding to a current density of 3×10^5 A/cm^2, would require the work function to be about 2.6 eV. Polycrystalline molybdenum has a work function of 4.35 eV,[15] and the types of contamination encountered in normal vacuum systems is likely to increase the work function. For example, a monolayer of oxygen adsorbed on molybdenum increases the work function by 1.5 eV, although nitrogen decreases the work function by 0.7 eV. However, it seems unlikely that the tip could have a work function as low as 2.6 eV, since this would require the adsorption of a highly electropositive material such as barium. If we assume that the area given by the current-voltage characteristic is correct, then the current density at 139 V would be 1.7×10^8 A/cm^2. Using this current density and the work function for clean molybdenum, 4.35 eV, we estimate from Dyke and Dolan's tabulation of the Fowler-Nordheim equation that the electric field at the surface would be 8×10^7 V/cm. This high field value would argue that the emitting atoms form a protuberance on the tip of the cone with a field magnification factor of 8/1.74 = 4.6. This magnification factor is close to that of a hemisphere on a plane which is 3.

Thus it is seen that the results are consistent with the hypothesis that the emission area is close to that given by the F/N method of Sec. III A and that the high field over a small area is caused by a protuberance on the tip. The results are inconsistent with the hypothesis that the tip is smooth and that the area reduction factor

TABLE II. Effect of changes of cathode dimensions in the 100-cone array. (Dimensions in μm.)

Cathode	x	r	D	V for 100 μA
17-13-15	0	0.050	1.3	120
17-18-1 E	0	0.050	1.7	180
17-18-1 I	0	0.060	1.9	225
17-13-15-F	+1.05	0.050	1.3	50
17-13-15 E	0	0.050	1.3	120
17-13-15 G	+0.14	0.050	1.3	80
17-13-20 G	−0.28	0.050	1.3	200
17-13-15 B	+0.84	0.065	1.9	100
17-18-1 I	0	0.060	1.9	225
17-18-1 H	+0.28	0.060	1.9	190
17-18-1 D	0	0.100	1.7	180
17-18-1 E	0	0.050	1.7	180
17-13-16 G	−0.075	0.050	1.6	125
17-13-16 H	−0.075	0.130	1.6	120

is explained by a linear work-function dependency on the field. This is because a smooth surface would require that the work function of the surface be 2.6 eV which is unreasonably low, and an area reduction factor of over 10^4 would require substantial deviation from the Fowler-Nordheim law which is not observed.

D. Effects of cathode dimensions on performance

The 100 emitter arrays were tested to ascertain the effect of change of geometry on the emission. The geometry was measured using the SEM and the emission was characterized by determining the voltage required to obtain 100 μA of emission current after the tube had stabilized. The SEM was also used to determine whether or not any tips were lost during processing. Some results grouped to illustrate the effects of three of the variables are given in Table II. In this table x is the distance of the tip above (+) or below (−) the lower plane of the gate electrode, and the other parameters, r and D, are as illustrated in Fig. 10. From these results, we see that the tip emission is strongly dependent on the diameter of the hole in the gate electrode [Fig. 11(a)] and on the position of the tip with respect to the lower plane of the gate electrode [Fig. 11(b)]. If the tip is made to protrude through the hole, the cathode can be made to operate at as low as 50 V to obtain an emission of 100 μA. One surprising aspect is that variation in the tip radius appears to have a second-order effect on the emission over the range 500—1500 Å.

The results indicate that protruding cones, with D as small as possible, should be used. However, as a practical limit, it has proved difficult to form cones that protrude through the hole in the gate electrode with values of D less than 1 μm without reducing the oxide thickness.

E. Maximum emission per cone

The current that can be drawn from an individual cone is limited by the initiation of a vacuum arc, which completely disrupts the top of the cone. Figure 12 shows the effect of a particularly violent disruption of a single cone in a 5000-cone array TFFEC. It will be noted that despite the splatter of material only one cone was affected and no chain of disruption events was set in

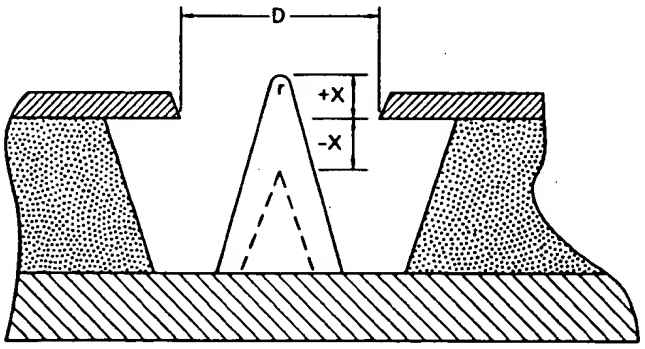

FIG. 10. Parameter definition.

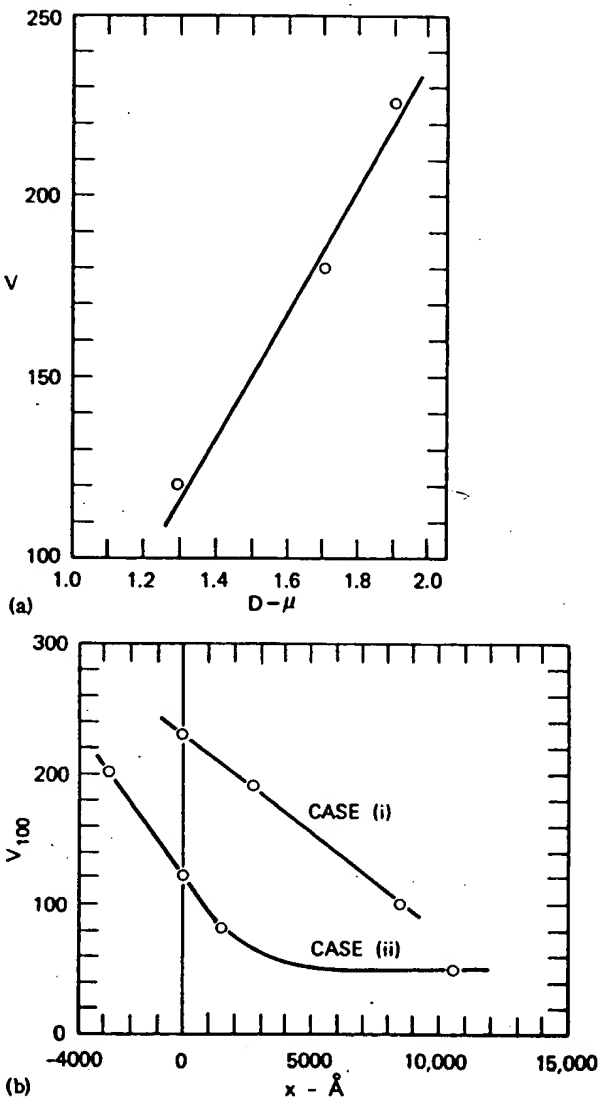

FIG. 11. (a) Voltage for 100 μA as a function of D; r = 500 Å, x = 0. (b) Voltage for 100 μA as a function of x. Case (i) r = 600 Å, D = 1.9 μm; case (ii) r = 500 Å, D = 1.3 μm.

FIG. 12. Disruption of a single cone in a 5000-array TFFEC.

motion. The conditions for this type of disruption have been discussed in a number of papers.[17,18] The currently accepted mechanism for this voltage range is that, provided there is no substantial release of gas due to electron bombardment of the anode causing a large increase in ambient pressure, disruption occurs when the hottest part of the cone approaches the melting point of the material of which it is composed. This is an unstable situation causing a runaway gasification of the tip analogous to an exploding wire. The temperature is governed by the heat-generating mechanisms of Joule heating and of the Nottingham effect,[19] and the heat-loss mechanisms of conduction down the shank and of radiation. The Nottingham effect tends to hold the emitting surface at a critical temperature T_c [20–23] where the energy lost to the surface by electrons tunneling from above the Fermi level is exactly balanced by the energy given up to the surface by electrons tunneling from below the Fermi level. To a close approximation T_c is given by

$$T_c = 5.32 \times 10^{-5} E/\phi^{1/2} \quad ^\circ\mathrm{K}. \tag{13}$$

The tips of TFFEC devices disrupt when the emission drawn from them is in the range 50—150 μA. If the larger area desired for the cone tip in Sec. III C is used, 50 μA corresponds to a current density of

$$J = (50 \times 10^{-6})/(6.3 \times 10^{-11}) = 8 \times 10^5 \quad \mathrm{A/cm^2}. \tag{14}$$

This current density with a work function of 2.6 eV would require $E = 2.2 \times 10^7$ V/cm giving $T_c \sim 790\,^\circ$K. On the other hand, if the smaller area is used, the current density is

$$J = (50 \times 10^{-6})/(1.2 \times 10^{-15}) = 4.1 \times 10^{10} \quad \mathrm{A/cm^2}.$$

This current density and a work function of 4.35 eV would require $E = 15 \times 10^7$ V/cm giving $T_c \sim 3800\,^\circ$K. The surface is always at a lower temperature than T_c because of the dominant effect of conduction.[21] Thus, to account for tip disruption caused by melting, use of the smaller emitting areas with the high T is indicated, since the melting point of molybdenum is 2893 °K.

IV. EMISSION STABILITY

A. General background

Time variations of emission from a source can be divided into four classes as follows:

(a) A slow deterioration in the average emission characteristics that takes place over long periods of time. This limits the useful life of the cathode, which may be defined by some arbitrary factor such as the time for the average emission at a given voltage to decrease by a chosen amount. For use in a microwave tube, cathode lives of from 10 000 to 100 000 h may be desirable. In demountable electron optical devices such as a scanning electron microscope, cathode lives of a few hundred hours may be acceptable.

(b) A sudden increase or decrease of emission which then remains unchanged for periods of time from 10^{-1} to 10^2 sec. These have been called "short-term fluctuations", and are observed mainly on the single-cone TFFEC's and the etched wires.

(c) A low-frequency noise containing frequencies in the range 10 Hz to 100 kHz. These fluctuations make up the "flicker" noise.

(d) The shot noise, which is directly related to the discrete nature of the electron and usually becomes dominant at frequencies above 100 kHz.

The single cones, the character of the flicker noise changes dramatically in bursts that last from 10^{-1} to 10^2 sec. These bursts are usually associated with the change of emission noted in (b). For arrays the superposition of the burst noise from individual cones causes the burstlike characteristic to be substantially modified (measured as a fraction of the total current). In the 100-cone arrays bursts are rarely seen, and the effect is essentially nondetectable in the 5000-cone arrays.

In Sec. IV B, measurements on these effects are discussed in more detail.

B. Life

Five single-cone TFFEC's were put on life test in a 50-l/sec ion-pumped system at a pressure of more than 10^{-9} Torr. Each TFFEC was operated continuously at a current of 1 μA with a collector potential of 120 V. During the initial measuring period, the gate potential for 1-μA emission dropped until a steady value (around 120 V) was reached. The cathodes then continued essentially unchanged for 3300 h when the life test was terminated.

Life tests were also made with three of the 100-cone arrays. These data were obtained in sealed tubes with a 2-l/sec ion appendage pump as shown in Fig. 13. The tubes were processed before they were sealed as described in Sec. II, with a pressure in the tube of about 10^{-9} Torr, as measured at the appendage pump. An alternating potential at a frequency of 60 Hz was applied to the gate that, by its action, produced a rectified cur-

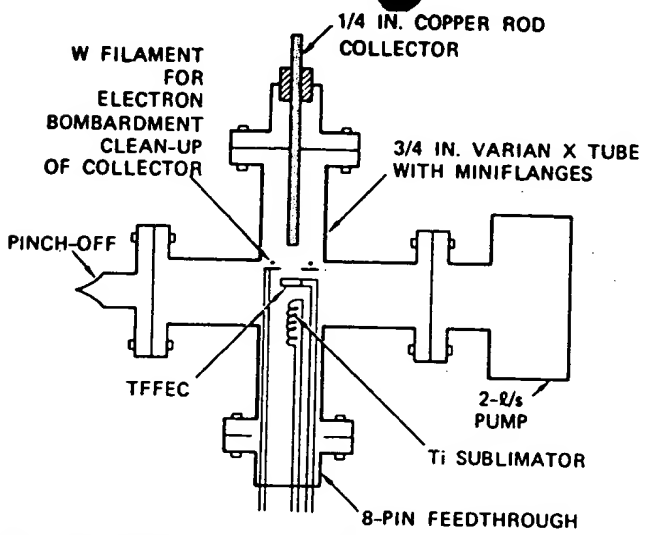

FIG. 13. Schematic of life test tube.

rent, thus reducing the anode dissipation. After an initial aging period of a few hundred hours the pressure reached a barely detectable level on the appendage ion pump, indicating a pressure of less than 10^{-9} Torr. The emission was held at a 2 mA peak corresponding to an average of 20 μA peak per cone and an overall peak current density of 3.2 A/cm^2. This was a stringent test, since the peak current per cone approached the disruption value. The results are shown in Fig. 14.

The collector power supply for each of the cathodes failed during the life test, causing the electron current to be collected by the thin molybdenum gate electrode. For two of the cathodes [see Figs. 14(a) and 14(b)] this event occurred early in life and both cathodes slowly but completely recovered from this experience over a period of about 1200 h of operation, indicating that the effect was most likely due to impurities released from the gate film being adsorbed on the cone tips rather than any changes in the geometry of the tips or the disruption of some of the cones, both of which would have caused a permanent change. Nevertheless both these cathodes showed evidence of a subsequent gradual decline of emission performance with time, amounting to about 10% in 7000 h of total life. The third [Fig. 14(c)] cathode had its anode supply fail after 4400 h of operation at which time it showed an erratic decline, but has remained stable at 1.2-mA emission for the last 1000 h. If Brodie's theory[3] of tip erosion by ion sputtering is applied, an approximate life of

$$L=\frac{2\times10^{-11}}{IP}=\frac{2\times10^{-11}}{(20\times10^{-6})(5\times10^{-10})}=2000\text{ h}$$

is obtained. This assumes a current of 20 μA per cone and a pressure of 5×10^{-10} Torr. This value of L is of the correct order of magnitude, bearing in mind that the ac voltage applied to the gate is rectified so that the cathode is actually operated for less than one-half the time.

On the other hand, the erratic decline for cathode 17-18-5E appeared to occur in steps, which argued that cone disruption in groups was taking place at the higher emission density per tip, at which this cathode was operating after the collector supply accident. For this reason, the gate voltage was reduced and although the total current was also reduced it has remained stable for a further 1000 h.

While much more work on cathode life is necessary before definitive conclusions can be made, lives of several thousand hours at overall emission densities of 3.2 A/cm^2 can be expected in good ion-pump vacua for the 100-cone TFFEC arrays.

Life tests on the 5000-cone arrays have been planned but no data are available at the time of this writing.

C. Short-term fluctuations

Figure 15 shows the types of short-term fluctuations typically observed with single-cone TFFEC devices, as recorded on a strip-chart recorder moving at the rate of 0.2 cm/sec. The cathode in this case was well aged by operating it for several hundred hours on a 500-l/sec ion-pumped system, which was monitored with a quadrupole mass spectrometer. During the entire experiment, the pressure was 10^{-10} Torr or better and the quadrupole showed that the residual gas was mainly

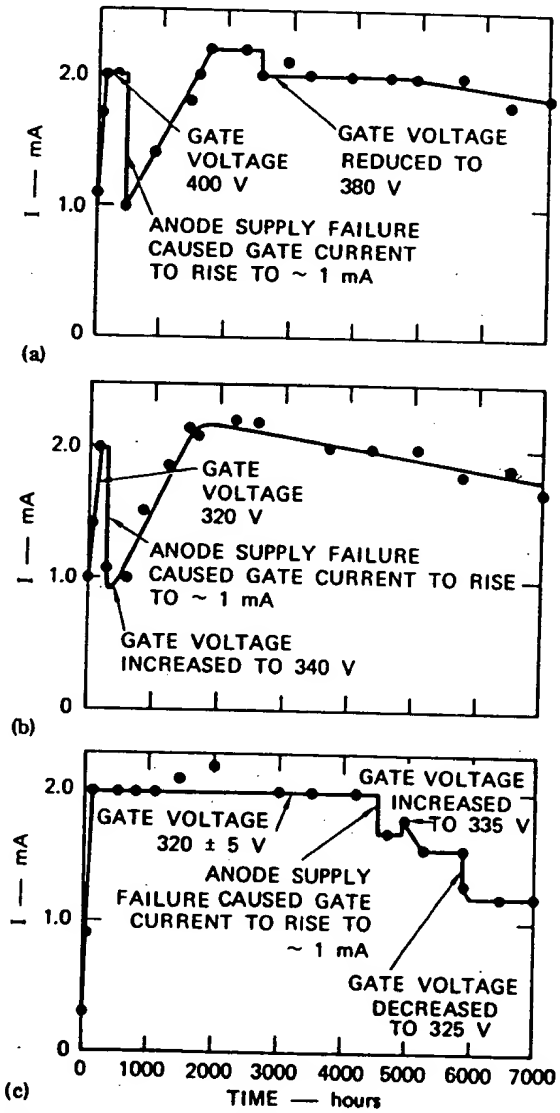

FIG. 14. Life test results: (a) cathode 17-13-17-D; (b) cathode 17-13-17-G; (c) cathode 17-18-5-E.

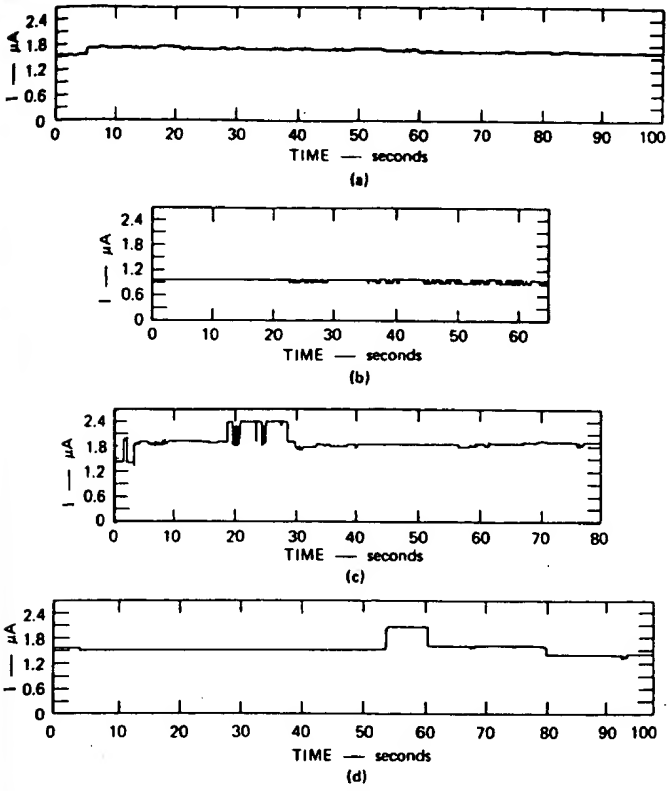

FIG. 15. Short-term fluctuations observed with single-cone TFFEC.

hydrogen. Nevertheless the current is rarely "steady", and is almost always showing bistable changes that appear to come in groups. The pulses within a group are usually of the same amplitude but the amplitude may vary from group to group. For example, in Fig. 15(c) where the average emission current was about 2 μA, large bistable changes of 0.5 μA or 25% of the average current were observed and lasted from 0.1 to 5 sec. A similar large-amplitude change is seen in Fig. 15(d). Figure 15(b) shows a clear bistable sequence of smaller amplitude 0.12 A at an average current of 1 μA, (i.e., a 12% fluctuation) that lasts from 0.1 to 2 sec. Note that even during the relatively quiescent period shown in Fig. 15(a), the changes are always in the form of steep sided steps (within the response time of the recorder.) Similar behavior is observed with the conventional etched point. With the 100- and 5000-cone arrays, the bistable character of the short-term fluctuations is lost and the variation of current with time has a more random appearance. Figure 16(a) shows a 100-cone array operating at 1 mA or 10 μA per cone; the rms deviation is about 1% indicating that the noise is caused by the fluctuations of individual cones, as is to be expected. For the 5000-tip array, the fluctuation of individual cones is always too small, compared with the total current, to be observed on this scale [Fig. 16(b)].

D. Burst noise

Burst noise has a waveform of bistable or multistable levels that can best be described as a nonstationary fluctuation superimposed on otherwise white noise.[24] It was first observed in the waveform of germanium point-contact diodes[25] and has subsequently been observed in tunnel diodes, resistors, forward- and reverse-biased p-n junctions, and junction transistors.[26]

Tunnel diodes are similar to the field emitters described in this paper, in that electrons are injected into the crystal lattice by field emission. In our field emitters, the electrons were injected into a vacuum and it was also found with the single-cone TFFEC's that bursts of bistable and multistable modes occurred. These bursts can usually be associated with the short-term fluctuations described above. The duration of a given burst can be from less than 1 sec to minutes, and the bursts can be followed by relatively quiescent periods within the same time range.

The noise bursts consisted of a series of current pulses, either positive or negative, superimposed on the constant operating current. The character of the pulse remains similar during a burst but sometimes varies from one burst to another. Observation of these pulses on an oscilloscope is limited by the time constant of the input circuit. In our initial experiments, this time constant was fairly large—on the order of 0.5 msec; this caused pulses of the form shown in Fig. 17(a). By using an FET source-follower amplifier, the input circuit time constant was reduced to less than 2 μsec. Oscillographs taken in this way [Fig. 17(b)] demonstrated that the pulses of Fig. 17(a) were actually composed of sequences of pulses of equal height whose duration varied from a value shorter than the new response time

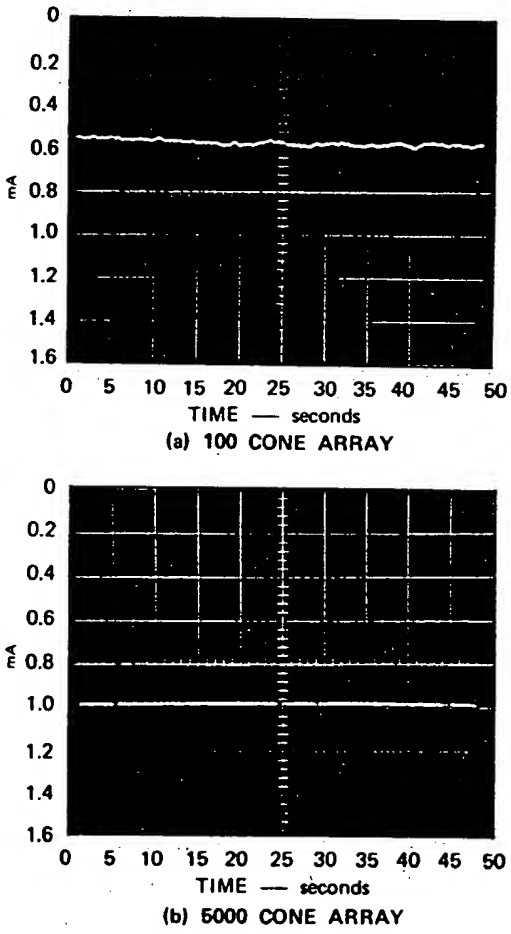

FIG. 16. Short-term current fluctuations from TFFEC array after 450°C bakeout and 100 h aging. (a) 100-cone array; (b) 5000-cone array.

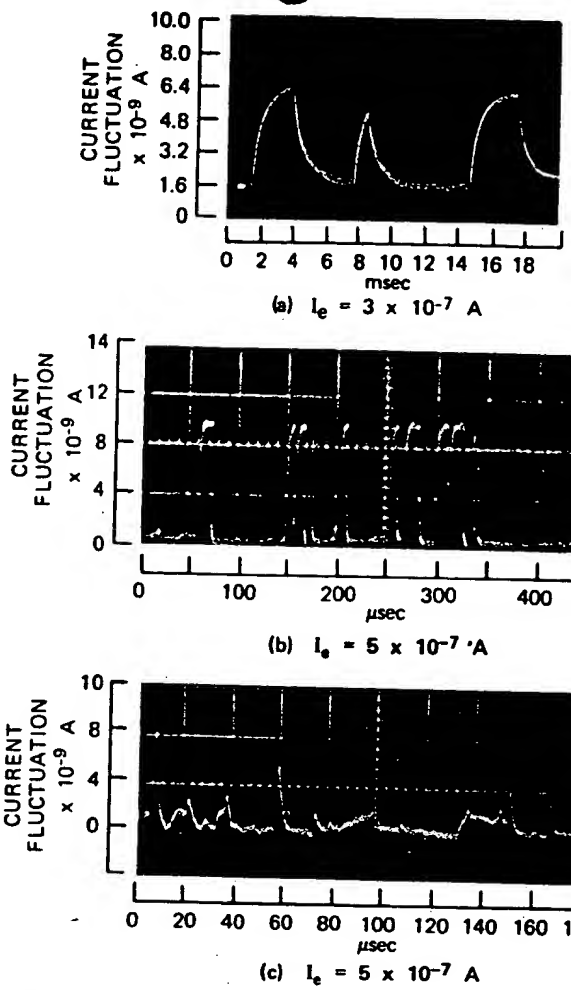

FIG. 17. Bursts of current pulses from single-cone TFFEC's.

(i.e., less than 2 μsec) to 20 μsec. These short pulses might consist of unresolved pulses of even shorter duration, but we have not been able to reduce the time constant further. These results were all obtained in the 500-l/sec ion-pumped system with well-aged cathodes operating in a vacuum of better than 10^{-10} Torr, the residual gas being mainly hydrogen.

The most striking facts about these bursts of pulses is that most are of equal height (or bistable) and come in groups, which can last for several milliseconds, although there is a random time distribution of pulses within the groups. Furthermore, the millisecond groups themselves come in bursts, with durations from fractions of a second to minutes.

When the amplitude of the basic (short) pulse is large but the duration of the pulse is less than the response time of the circuit, the pulse appears as a spike with a sharp front and a characteristic decay. The fact that the circuit has not fully responded means that the peak does not represent the full height of the pulse, and in certain modes, this effect causes the trace to have a more random appearance [Fig. 17(c)]. However, it seems likely that sufficient time resolution would show these pulses to be of equal height.

The superposition of the short pulses from individual cones makes the burst effect less distinctive in the arrays, although it is still observable. However, in this respect the etched wires behave similarly to the single cones.

E. Flicker noise spectra

Figure 18 gives a schematic diagram of the equipment used to measure the noise spectra in the range 100 Hz to 100 kHz. The cathodes were all operated in the 500-l/sec ion-pumped system described above at pressures below 10^{-10} Torr with the residual gas being mainly hydrogen. It was necessary to measure the noise output at the different frequency ranges contemporaneously to avoid the effects caused by sudden changes in noise properties, particularly those shown in the single-cone cathodes.

Eight fixed-frequency high-Q bandpass filters were constructed with center frequencies of 100, 250, 500,

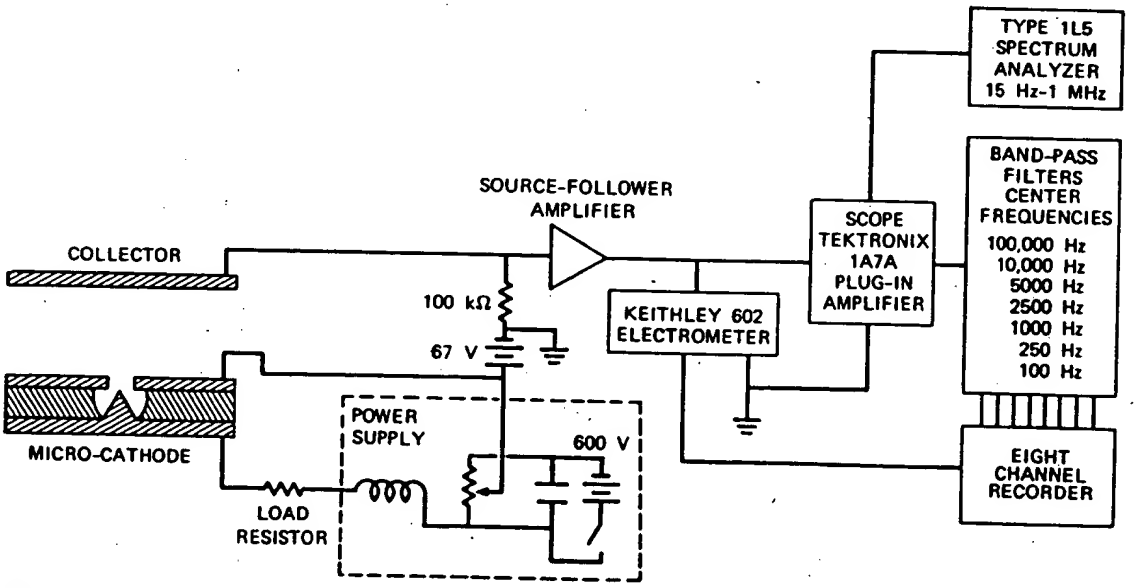

FIG. 18. Noise measurement system.

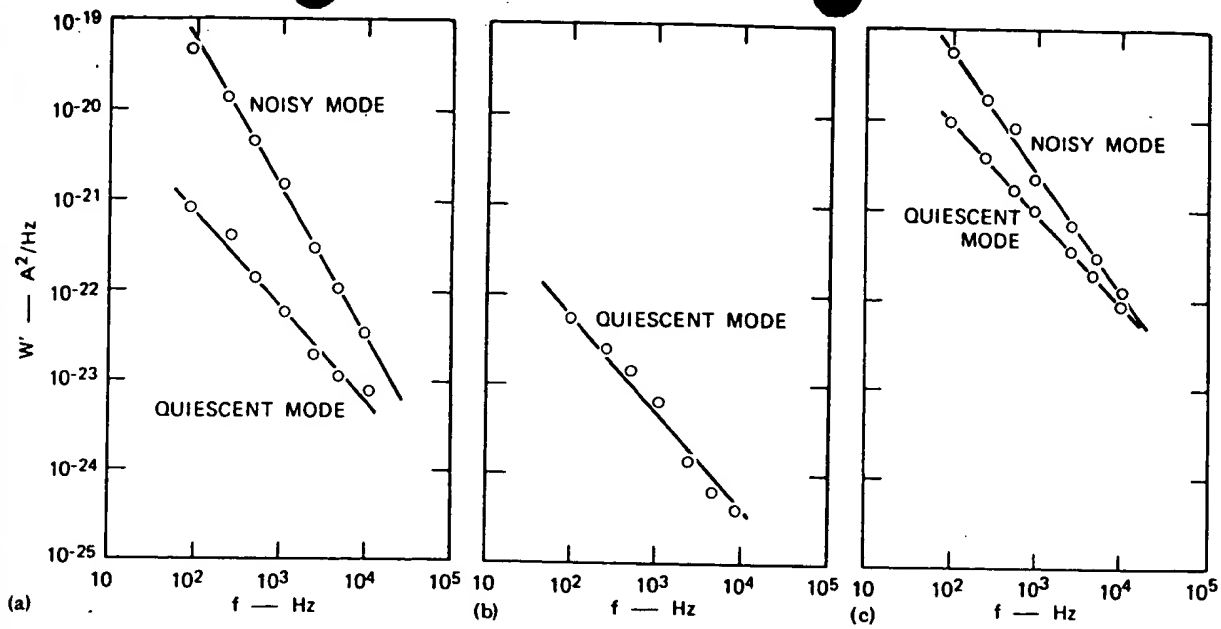

FIG. 19. Noise spectra for single-cone TFFEC (18-11-2T). (a) $I = 2\times10^{-7}$ A, W' for shot noise $(2eI) = 6.4\times10^{-26}$ A²/Hz; (b) $I = 4.5\times10^{-6}$, W' for shot noise $= 1.4\times10^{-26}$ A²/Hz; (c) $I = 1.5\times10^{-6}$, W' for shot noise $= 4.8\times10^{-25}$ A²/Hz.

1000, 2500, 5000, and 10 000 Hz. A Tektronix IL5 was used as the 100 000-Hz filter. In addition, a Tektronix IL5 spectrum analyzer was used for monitoring the overall spectral distribution. The output impedance of the measurement circuit was too high to achieve good frequency response above 5000 Hz. However, the addition of an FET source-follower amplifier placed between the collector and the noise measurement equipment extended the flat frequency response to 500 kHz. The output of each bandpass filter was fed into an averaging circuit with a time constant of 10 sec, then into a channel of an eight-channel recorder. The recorded signal was thus proportional to the average rms value of the signal at the frequency of the filter. The system was calibrated using a saturated thermionic diode as a shot noise source and checked using sine waves of known amplitude.

In general, the flicker noise is described by the mean square current fluctuation $\langle i_F^2\rangle_{av}$ at a given frequency f in a given frequency range Δf when held at an average current I.

In general

$$\langle i_F^2\rangle_{av} = A\,W(f,J)\Delta f \tag{15}$$

$$= W'(f,I)\Delta f, \tag{16}$$

where A is the emitting area, J is the average current density, and W is the noise intensity distribution function. The objective of the measurements is to obtain W as a function of f and J. As outlined in Sec. III C, the estimation of the emitting area is open to differing interpretations. For this reason, we use Eq. (16) for the empirical description of the flicker noise. Plots of W' versus f at various values of I are obtained for each cathode.

Results for the single-cone cathode (18-11-2T), used for the previously illustrated Fowler-Nordheim plot, are shown in Fig. 19. In general, the spectrum differs

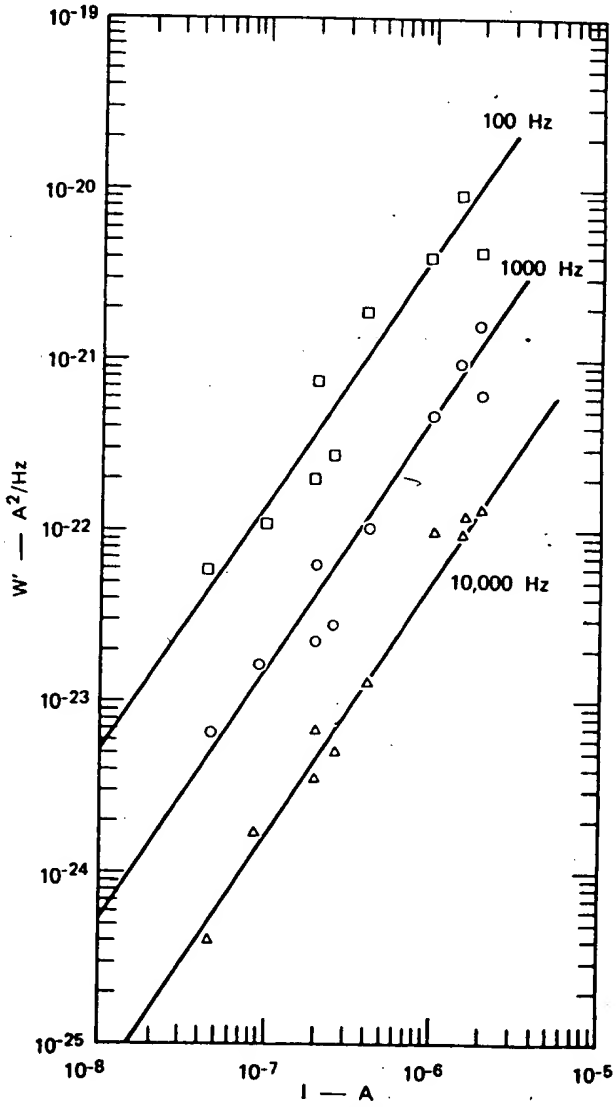

FIG. 20. Noise as a function of current for single-cone TFFEC in quiescent mode (18-11-2T).

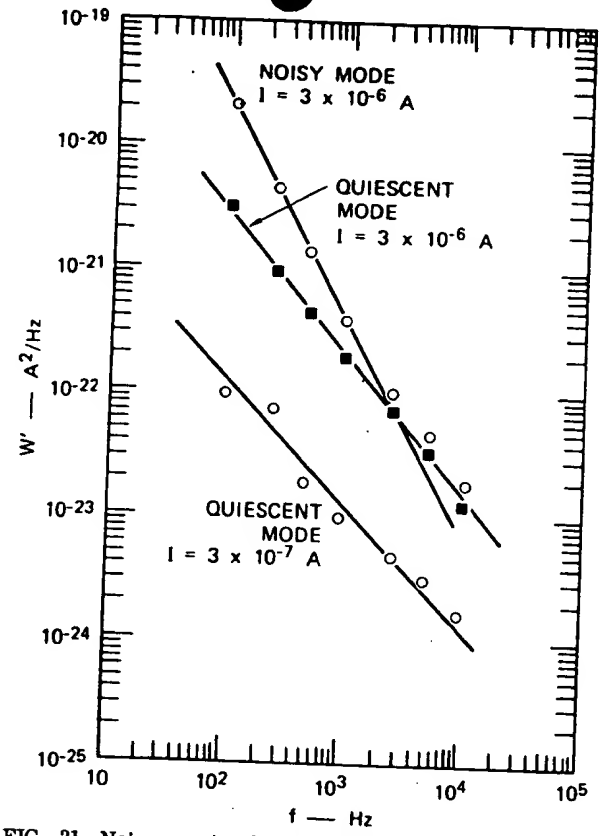

FIG. 21. Noise spectra for etched molybdenum points. (a) $I = 3\times10^{-6}$ A, (b) $I = 3\times10^{-7}$ A.

from mode to mode and the figure shows the spectra for the noisiest and the most quiescent modes at different current levels. Usually the most quiescent mode showed a spectrum close to $1/f$ and a current variation close to $I^{1.5}$ (Fig. 20). The noisiest mode showed a spectrum closer to $1/f^2$ and was not strongly dependent on the current over the measured range (4.5×10^{-8} to 1.5×10^{-6} A). The current range was bounded at the lower end by the sensitivity of the noise neasuring apparatus and at the high end by the desire to avoid any instabilities that might occur as the cone disruption current was approached.

The fact that the noise is not strongly dependent on the current in the noisiest mode is most extraordinary. The circuit was carefully checked to see that this noise was not being injected from some spurious source. Among other tests the field emission triode was replaced with a low-noise metal-film resistor to emulate the same operating conditions in the circuit. In the latter case, the noise was reduced to a very low level, and no evidence was observed to explain the existence of high noise bursts. Hence, we concluded that it was a genuine property of the field emitting source. Even in the "quiescent" mode, the flicker noise is many orders of magnitude above the shot noise in the frequency range measured for that current.

The etched molybdenum wire cathodes showed similar behavior (Fig. 21), with the noisiest mode roughly proportional to $1/f^2$ and the quiescent mode to $1/f$. The noisiest mode appeared to be somewhat quieter than the noisiest mode of the single cone and did not appear until currents of 5×10^{-7} A were drawn. For the quiescent mode, the noise versus current behavior (Fig. 22) is also similar to the single-cone TFFEC, being proportional to $I^{1.5}$ (Fig. 22) except that the noise from the etched wire is a factor of 10 smaller for a given current. If we use Eq. (1) to describe the noise and assume that the emitting surfaces are similar in both cases, we obtain

$$W_c' = A_c W(f, I/A_c) \tag{17}$$

and

$$W_E' = A_E W(f, I/F_E), \tag{18}$$

where c refers to the single-cone TFFEC and E to the etched molybdenum wire. If we further assume that $W\alpha(J^x/f^y)$, then

$$\frac{W_c'}{W_E'} = \frac{A_c}{A_E}\left(\frac{A_E}{A_c}\right)^x. \tag{19}$$

From the measurements shown in Fig. 22 we obtain $x = 1.5$, and $W_c'/W_E' = 10$, hence $A_E/A_c = 10^2 = 100$. This compares with a ratio obtained by the Fowler-Nordheim method (see Table I) for the same cathodes of 55. Bearing in mind the spread in the data from which these results were derived, agreement within a factor of 2 seems reasonable and supports the idea that the correct emitting areas are given by the Fowler-Nordheim method.

The spectra for the 100-cone arrays also show mode behavior, but the modes are not so sharply separable and exhibit curious spectra, as illustrated in Fig. 23. Presumably, each individual cone can be in a quiescent or noisy mode at different times, and the sum of the

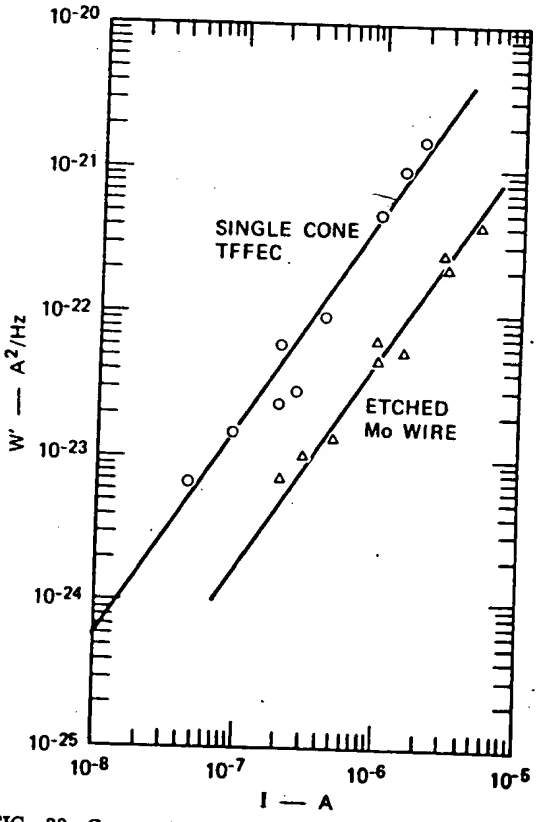

FIG. 22. Comparison of noise as a function of current at 1000 Hz for the single-cone TFFEC (18-11-2T) and the etched molybdenum point.

TABLE III. Comparison of flicker noise spectra for various field emission cathodes.

Cathode	Current range (A)	Frequency range	y	x	Ref.
Clean single-crystal tungsten	4.5×10^{-7} to 1.2×10^{-5}	100 Hz to 10 kHz	0.75	2	27
Tungsten with adsorbed residual gases	3.2×10^{-7} to 2.6×10^{-6}	100 Hz to 10 kHz	1—1.3	• • •	27
Tungsten with adsorbed barium	1.4×10^{-8} to 8×10^{-7}	100 Hz to 10 kHz	1.2—1.4	1	27
Tungsten with adsorbed potassium	6×10^{-7} to 2×10^{-6}	100 Hz to 10 kHz	1.2	1.86	29
Zr/W at 900—1576°K	10^{-8} to 10^{-7}	2—10 kHz	1—1.3	2.2	30
TFFEC molybdenum single cone (quiescent mode)	10^{-8} to 10^{-5}	100 Hz to 10 kHz	1	1.5	• • •
Etched molybdenum wire (quiescent mode)	10^{-7} to 10^{-5}	100 Hz to 10 kHz	1	1.5	• • •

noise currents from each is stationary for long enough to take a spectrum in a given condition. Figure 24 shows spectra for the 5000-cone array when operating at a current of 8.6×10^{-4} or 1.72×10^{-7} A per cone. Spectra were taken in the noisiest mode, in the quietest mode, and when elevated to a temperature of 275 °C. The character of the spectrum essentially remains the same regardless of its condition. Up to about 5000 Hz, the spectrum shows a $1/f^2$ characteristic. However, at around 5000 Hz, a new noise source, generated in the system, begins to become effective, which increases with increasing frequency, with a broad peak covering 50—100 kHz. Figure 25 shows that the current dependency of the noise in the $1/f^2$ portion of the spectrum is proportional to I, but proportional to I^2 at 100 kHz where the new noise source has become dominant. Note that there is no evidence for the existence of this new noise source in either the single- or 100-cone array. In the low-frequency half of the spectrum for the 5000-cone array, the total noise appears to be dominated completely by the cones in the noisy mode, since they always show a close to $1/f^2$ spectrum.

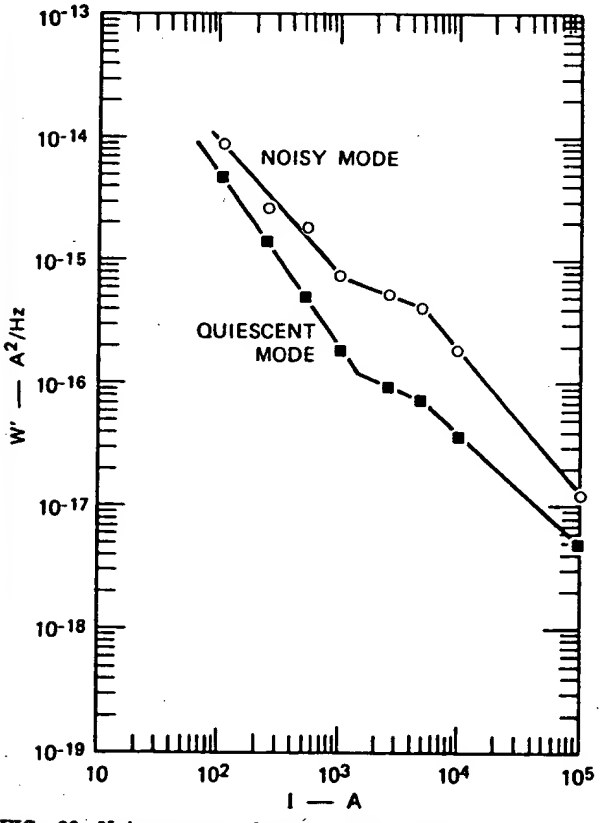

FIG. 23. Noise spectra for 100-cone array TFFEC (17-13-19F) at $I=5.04\times10^{-4}$ A (where W' for shot noise $=1.6\times10^{-22}$ A²/Hz).

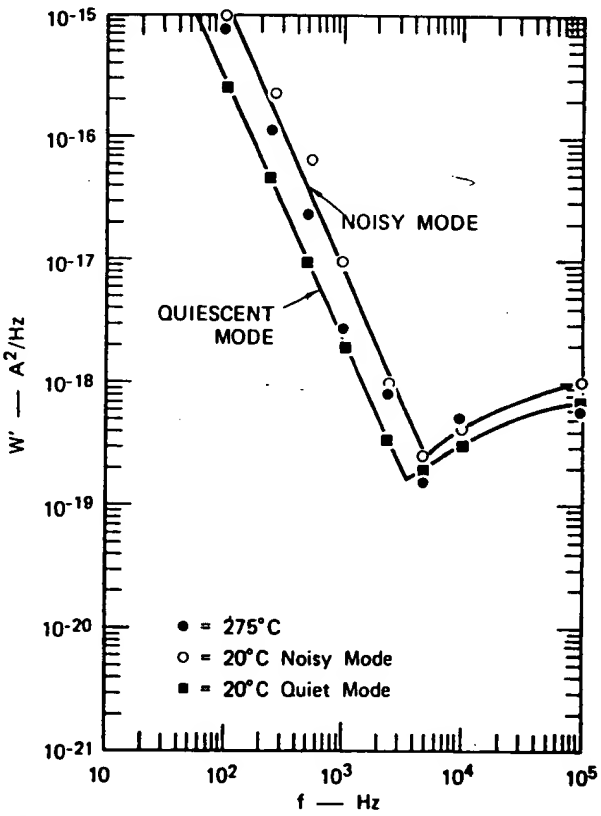

FIG. 24. Noise spectra for 5000-cone array TFFEC (20-6-1H) at $I=8.6\times10^{-4}$ A (where W' for shot noise $=2.75\times10^{-22}$ A²/Hz).

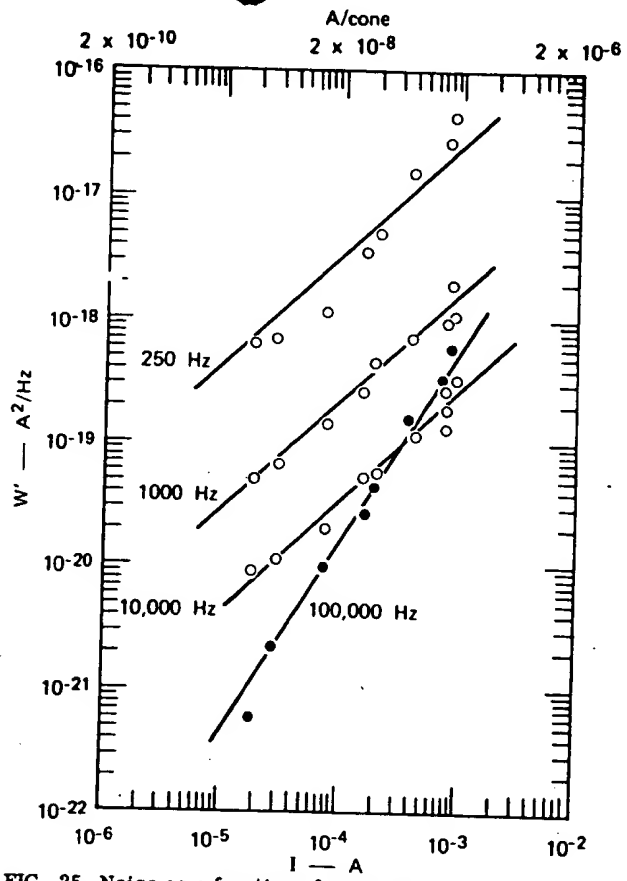

FIG. 25. Noise as a function of current for 5000-cone array TFFEC (20-6-1H).

In the case of the 5000-cone array, the difference in modes must be caused by the change in the number of cones in the noisy mode, since the contribution of the cones in the quiescent mode make a much smaller contribution to the total noise. The fact that the noise at a given frequency as a function of current shows a linear variation argues that the probability of the cone being in the noisy mode is proportional to the current being drawn from it. If all the cones were in the noisy mode at a level measured from the single-cone experiment, a saturation in noise would be expected when all the cones are in their noisiest state. Extrapolation of the data in Fig. 25 suggests that this would occur at about 3.5 mA when the noise would be 5000 times that of the single cone in its noisiest mode at a corresponding frequency. Unfortunately, the power limitation of the collector prevented these current levels from being reached on a continuing basis to check for this effect. However, at 2×10^{-7} A per cone the hypothesis suggests that about 30% of the cones are in the noisy mode at any given time, or each cone spends about one-third of its time in the noisy mode when drawing this current. Chart recordings of the single cone operating at 2×10^{-7} A showed that in a 300-sec (5-min) period it was in the noisiest mode for about 100 sec (comprised of three bursts each of approximately 30—40 sec duration). This result is consistent with the suggested explanation of the behavior of the 5000-cone array at the low-frequency end. The fact that the noise at the high-frequency end (100 000 Hz) increases as the square of the current demonstrates that its mechanism of generation is totally different from that at the low-frequency end of the spectrum.

Other investigators have studied field emission flick noise,[27–30] but, unfortunately, none using molybdenum cathodes. No mention of the mode behavior reported here has been made even on contaminated points, and no data has been given from which the emission area could be estimated. However, the flicker noise showe the usual variations with frequency and current, when the shot noise had been subtracted, taking the form

$$\langle i_F^2\rangle_{av} \alpha I^x/f^y. \qquad (2$$

A comparison is given in Table III.

V. THE NATURE OF THE EMITTING SURFACE

The evidence given in this paper indicates that emission from the tip of the cones of the TFFEC arises fro just one or a few atoms located on the tip. This eviden is summarized as follows:

(a) The areas given by the Fowler-Nordheim method are of the order of a few unit cell dimensions (Sec. III C).

(b) The electric fields at the tip, assuming a smooth spherical cap, are too small by a factor of 4 to accoun for the observed field emission without requiring an unreasonably low work function for the surface. The necessary enhancement factor is of the right order to be accounted for by an adsorbed molecule (Sec. III C).

(c) The apparent area reduction factor to be expected on the basis of a linear variation of work function with field is too large to be obtained without substantial deviation from the Fowler-Nordheim relationship. No such deviation is observed with the single-cone TFFEC (Sec. III C).

(d) Disruption of the cones at high current requires that the critical temperature of the Nottingham effect be above the melting point of molybdenum. This only occurs if the small areas given by the Fowler-Nordhei method is used (Sec. III E).

(e) The images observed in the field emission micro scope for the single-cone TFFEC consists of one or a few "lobes" that show no regular pattern, as is usually observed with the larger single-crystal faces of conventional thermally grown points (Sec. II). The lobes are mobile. The resolution and interpretation of such lobes as images of atoms is consistent with work by Rose,[31] Becker[32] and others, as critically reviewed by Dyke and Dolan[33] and Good and Mueller[34]; and by studie of field emitting whiskers.[35]

(f) The equal heights and rapid rise times of the burs of current pulses in all the time domains studied (Secs IV C and IV D) indicate the effect of single atoms, such as the rearrangement of atoms at the tip, the arrival and departure of atoms at the emitting area (by surface migration, solid diffusion from within the cone or arrival and departure to the vacuum external to the tip, or a change in the vibrational state of the adsorbed atom. The last change would alter the average distance from the surface of the adsorbed atom in a manner analogous to the nuclear separation of the diatomic

molecule and would thus cause a small local work-function change. The small-amplitude high-frequency pulses could arise from this source and the less common large-amplitude events from the gross movement of atoms from site to site.

(g) An alternative explanation worth discussing is the possibility that microneedles or whiskers are formed on the tips of the molybdenum cones similar to those recently reported by Okoyama,[36] who obtained dendritic growth on tungsten by the reduction of tungsten oxide. The dendrites were grown on 10-μ-diam tungsten wire; however, the ends of the whiskers were of similar dimensions to those of the cones grown in the experiments reported in this paper, having a tip radius of curvature in the range 0.05—0.2 μ. In other words, the tips of Okoyama's whiskers corresponded to the tips of the vapor-grown cones reported here. It seems unlikely that additional whiskers can grow from tips with radii of only 0.05 μ (or about 100 lattice spacings) since such whiskers would have to be only a few lattice spacings in diameter and a few atom spacings high to account for the observed field magnification factor. Thus, it would be a matter of semantics as to whether such protrusions were described as atomic bumps or whiskers. Considerable theoretical and experimental work has recently been done to explore the vibration spectra of adsorbed molecules by observing the energy distribution of field emitted electrons. A review of this technique called FEED has recently been given by Gadzuk and Plummer.[37] There can be no doubt as to the existence of an effect due to vibrational levels particularly at the temperatures that are likely to exist at the field emitting area.

Note added in proof. Life tests with the 100-cone arrays drawing 2 mA total emission (or 3 A/cm^2) have now continued in excess of 12 000 h as of October 1976.

ACKNOWLEDGMENTS

The work reported in this paper was done with support from the U.S Army Research Office, Durham, N.C., under Contract No. DAHC04-73-C-0007, and from the National Aeronautical and Space Agency, Lewis Research Center, Cleveland, Ohio, under Contract No. NAS3-18903. The work reported in this paper has benefitted from discussions and inputs from other past and present colleagues of the SRI Physical Electronics Group. The authors particularly wish to thank John Kelly for valuable discussions on the noise studies and for preparing the computer programs used in Sec. III E and Clifford C. Hartelius for advice in the materials science field. The field emission devices could not have been made without the outstanding microfabrication, design, and constructional skills of Robert D. Stowell and the diligent technical assistance of Hazel Pakka and Earl Heydon.

[1]C.A. Spindt, IEEE Conf. on Elec. Devices and Tech., New York 1973 (unpublished).
[2]C.A. Spindt, K.R. Shoulders, and L.N. Heynick, U.S. Patents 3,755,704 (1973), 3,789,471 (1973), 3,812,559 (1974).
[3]I. Brodie, Int'l J. Electron. 38, 541 (1975).
[4]A.H.W. Beck, Proc. IEE 106B, 372 (1959).
[5]A.S. Grove, *Physics and Technology of Semiconductor Devices* (Wiley, New York, 1967), p. 22.
[6]W.S. De Forest, *Photoresist* (McGraw-Hill, New York, 1975), p. 223.
[7]L. Heynick, E.R. Westerberg, C.C. Hartelius, Jr., and R.E. Lee, IEEE Trans. Electron Devices ED-22, 400—409 (1975).
[8]R.H. Fowler and L.W. Nordheim, Proc. R. Soc. London A 119, 173 (1928).
[9]R.E. Burgess, H. Kromer, and J.M. Houston, Phys. Rev. 90, 515 (1953).
[10]A. Van Oostrom, J. Appl. Phys. 33, 2917 (1962).
[11]E.M. Charbonnier and E.E. Martin, J. Appl. Phys. 33, 1897 (1962).
[12]W.P. Dyke and W.W. Dolan, Adv. Electron. Electron Phys. 8, 180 (1956).
[13]I. Brodie, J. Appl. Phys. 35, 2324 (1964).
[14]M. Abon and S.J. Teichner, Nuovo Cimento Suppl. 5, 521 (1967).
[15]G.A. Haas, *American Institute of Physics Handbook*, 3rd ed. (McGraw-Hill, New York, 1972), pp. 9—172.
[16]R. Gomer, *Field Emission and Field Ionization* (Harvard University Press, Cambridge, Mass., 1961).
[17]D. Alpert, P.A. Lee, and H.E. Tomasche, J. Vac. Sci. Technol. 1, 34 (1964).
[18]P.S. Chatterton, Proc. Phys. Soc. London 88, 231 (1966).
[19]W.E. Nottingham, Phys. Rev. 59, 907 (1941).
[20]P.H. Levine, J. Appl. Phys. 33, 582 (1962).
[21]I. Brodie, Int. J. Electron. 18, 223 (1965).
[22]F.M. Charbonnier, R.W. Strayer, L.W. Swanson, and E.E. Martin, Phys. Rev. Lett. 13, 397 (1964).
[23]D.A. Lee, University of Illinois Coordinated Science Laboratory Report R-280, 1966 (unpublished).
[24]W.H. Card and A. Mavretic, Second Symp. on the Physics of Failure in Electronics Chicago, 1963, Vol. 2, p. 268 (unpublished).
[25]R.G. Pay, thesis (University of Birmingham, 1956) (unpublished).
[26]S.T. Hsu, R.J. Whittier, and C.A. Mead, Solid-State Electron. 13, 1055 (1970).
[27]G.W. Timm, and A. Van der Ziel, Physica 32, 1333 (1966).
[28]Ch. Kleint, Surf. Sci. 25, 394 (1971).
[29]Ch. Kleint, R. Meclewski, and R. Blaszczyszyn, Physica 68, (1973).
[30]L.W. Swanson and N.A. Martin, J. Appl. Phys. 46, 2029 (1975).
[31]D.J. Rose, J. Appl. Phys. 27, 215 (1956).
[32]J.A. Becker, Bell Syst. Tech. J. 30, 907 (1951); J.A. Becker and R.G. Brandes, J. Appl. Phys. 27, 221, (1956).
[33]See Ref. 12, pp. 132—137.
[34]R.H. Good and E.W. Mueller, *Handbuck der Physik* (Springer-Verlag, Berlin, 1956), Vol. 21, p. 176.
[35]I. Brodie, J.Vac. Sci. Technol. 2, 249 (1965).
[36]F. Okuyama, J. Vac. Sci.Technol. 12, 1399, (1975).
[37]J.W. Gadzuk and E.W. Plummer, Rev. Mod. Phys. 44, 487 (1973).